Supplementary Information

including

Supplementary Figures 1-15
Supplementary Table 1

for

Conformational Coupling Between Extracellular and Transmembrane Domains Modulates Holo-adhesion GPCR Function

Szymon P. Kordon[1, 2, 3, 4, #], Kristina Cechova[5, #], Sumit J. Bandekar[1, 2, 3, 4], Katherine Leon[1, 2, 3, 4], Przemysław Dutka[1, 6], Gracie Siffer[5], Anthony A. Kossiakoff[1], Reza Vafabakhsh[5, *], Demet Araç[1, 2, 3, 4*]

1 Department of Biochemistry and Molecular Biology, The University of Chicago, Chicago, IL, USA

2 Neuroscience Institute, The University of Chicago, Chicago, IL, USA

3 Institute for Biophysical Dynamics, University of Chicago, Chicago, IL, USA

4 Center for Mechanical Excitability, University of Chicago, Chicago, IL,

5 Department of Molecular Biosciences, Northwestern University, Evanston, IL, USA

6 Current affiliation: Department of Structural Biology, Genentech, South San Francisco, CA, USA

# These authors contributed equally to this work

* Correspondence: arac@uchicago.edu and reza.vafabakhsh@northwestern.edu

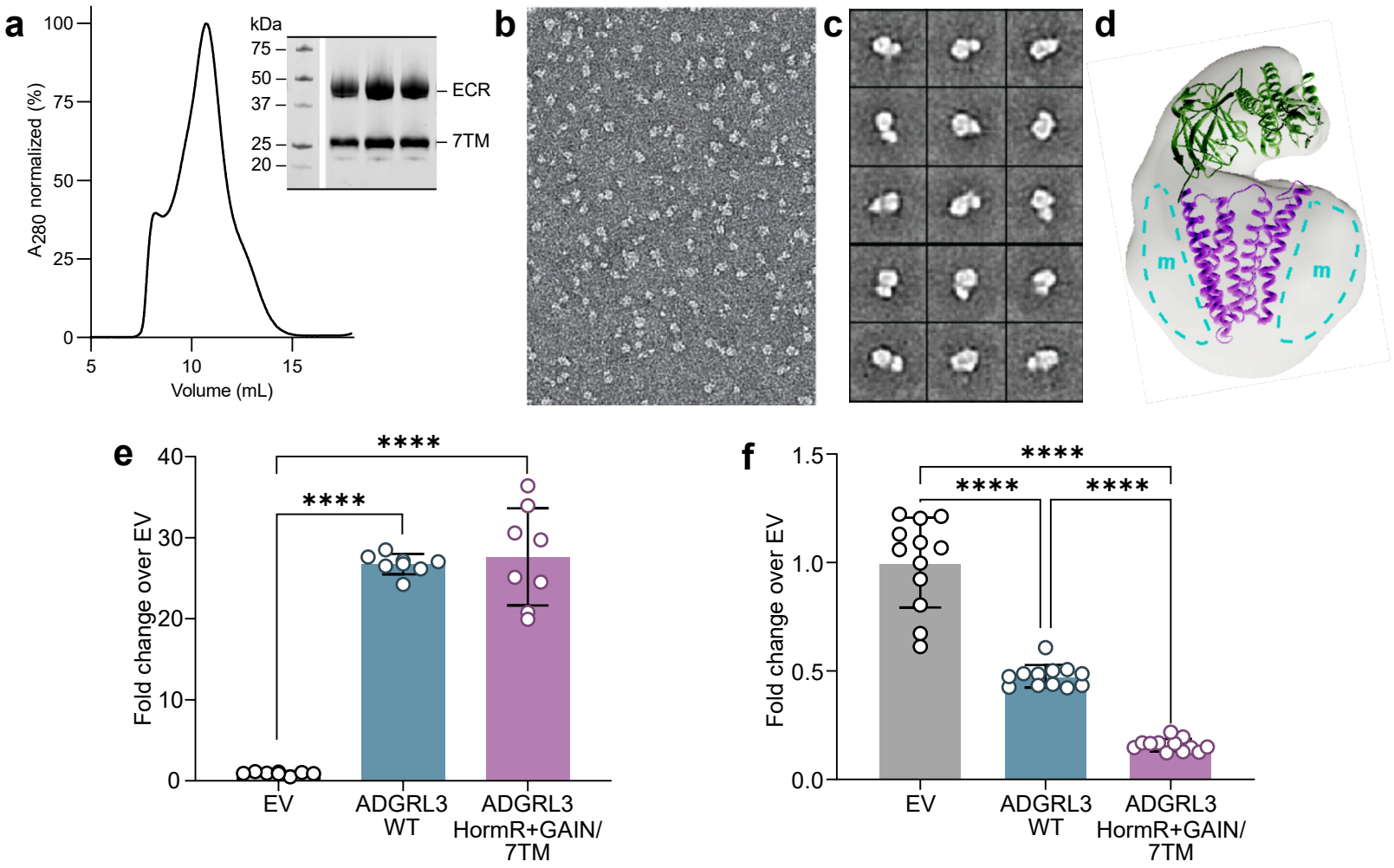

Supplementary Fig. 1: Purification of ADGRL3$_{HormR+GAIN/7TM}$ and validation of downstream signaling activity.

a SEC profile and SDS-PAGE analysis of the ADGRL3 holoreceptor purified in detergent. **b** Representative negative stain EM micrograph of purified ADGRL3 holoreceptor sample. **c** Representative negative stain EM 2D class averages of purified ADGRL3 in detergent micelle. **d** Low-resolution negative stain EM map of ADGRL3 in detergent micelle. Available structures of GAIN and 7TM domains placed manually in the density. **e** ADGRL3$_{WT}$ and ADGRL3$_{HormR+GAIN/7TM}$ signaling measured by the SRE-luciferase assay. Data are shown as a fold change over EV. Data are presented as mean ± SD of three independent experiments (n = 8); one-way ANOVA. **f** ADGRL3$_{WT}$ and ADGRL3$_{HormR+GAIN/7TM}$ signaling measured by the cAMP assay. Data are shown as a fold change over EV in the ADRB2 background. Data are presented as mean ± SD of three independent experiments (n = 12); one-way ANOVA.

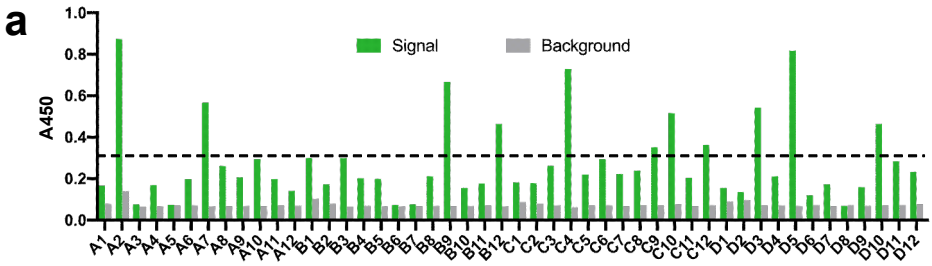

b

sAB ID	ADGRL3					
	HormR/GAIN			Full ECR		
	k_{on} ($M^{-1}s^{-1}$)	k_{off} (s^{-1})	K_D (nM)	k_{on} ($M^{-1}s^{-1}$)	k_{off} (s^{-1})	K_D (nM)
LK1	1.3×10^5	4.3×10^{-4}	3.3	1.2×10^5	4.8×10^{-4}	4.0
LK3	4.5×10^5	1.7×10^{-3}	3.9	3.5×10^5	1.9×10^{-3}	5.4

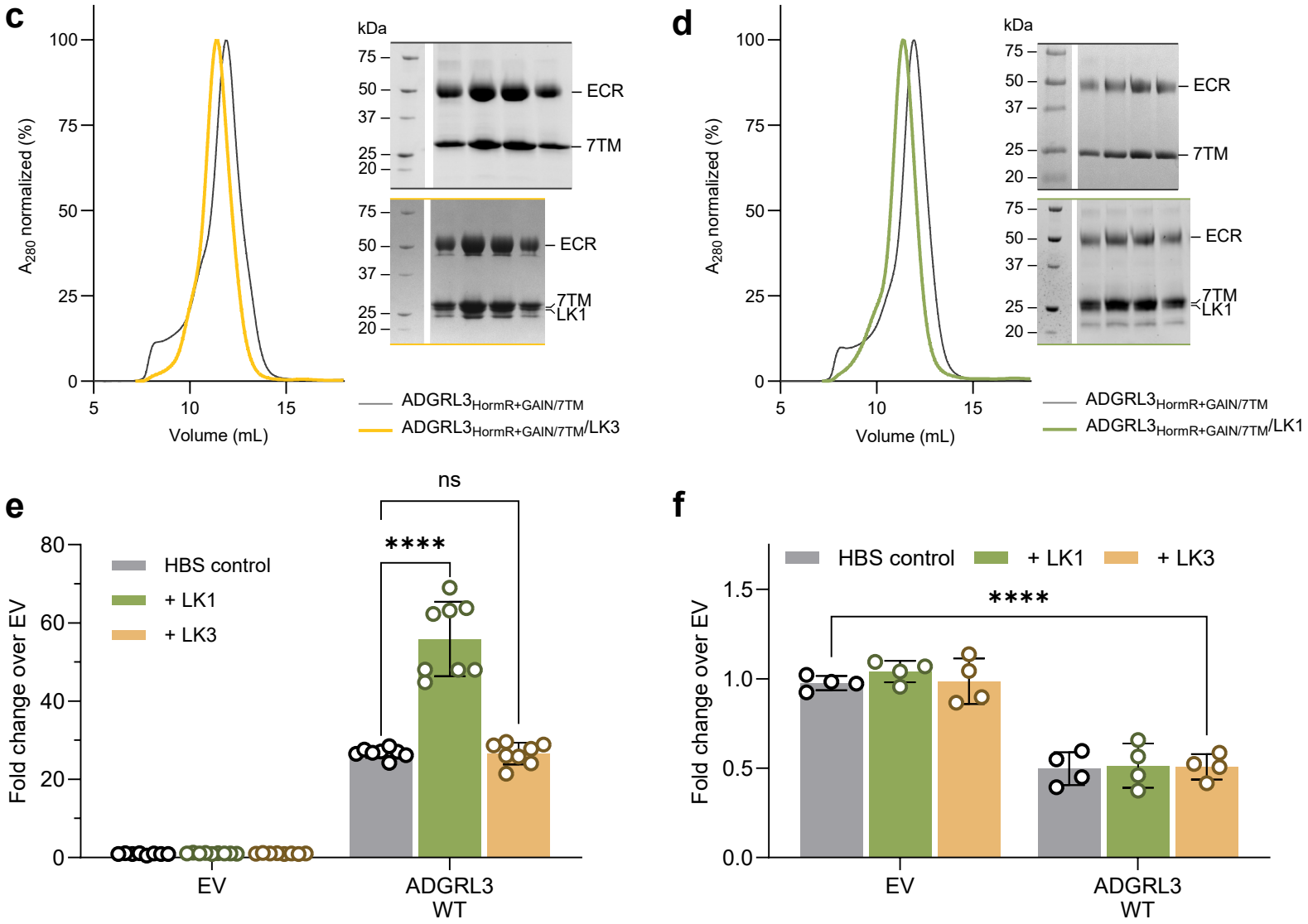

Supplementary Fig. 2: Synthetic antigen binders generation and validation

a Representative results of single point phage ELISA for sABs against ADGRL3 HormR/GAIN fragment. **b** Kinetic values of sABs LK1 and LK3 developed against HormR/GAIN domains of ADGRL3 obtained by SPR. **c** and **d** SEC profiles and SDS-PAGE analyses show both LK3 (c) and LK1 (d) forming monodisperse complexes with the purified ADGRL3 in detergent micelle. **e** ADGRL3 signaling measured by the SRE-luciferase assay in the presence of 2 µM of LK1 or LK3. Data are presented as a fold change over EV. Data are presented as mean ± SD of three independent experiments (n = 8); sAB vs. HBS buffer treatment; two-way ANOVA. **f** ADGRL3 signaling measured by the cAMP assay in the presence of 2 µM of LK1 or LK3. Data are shown as a fold change over EV in the ADRB2 background. Data are presented as mean ± SD two independent experiments (n = 4), sAB vs. HBS buffer treatment; two-way ANOVA.

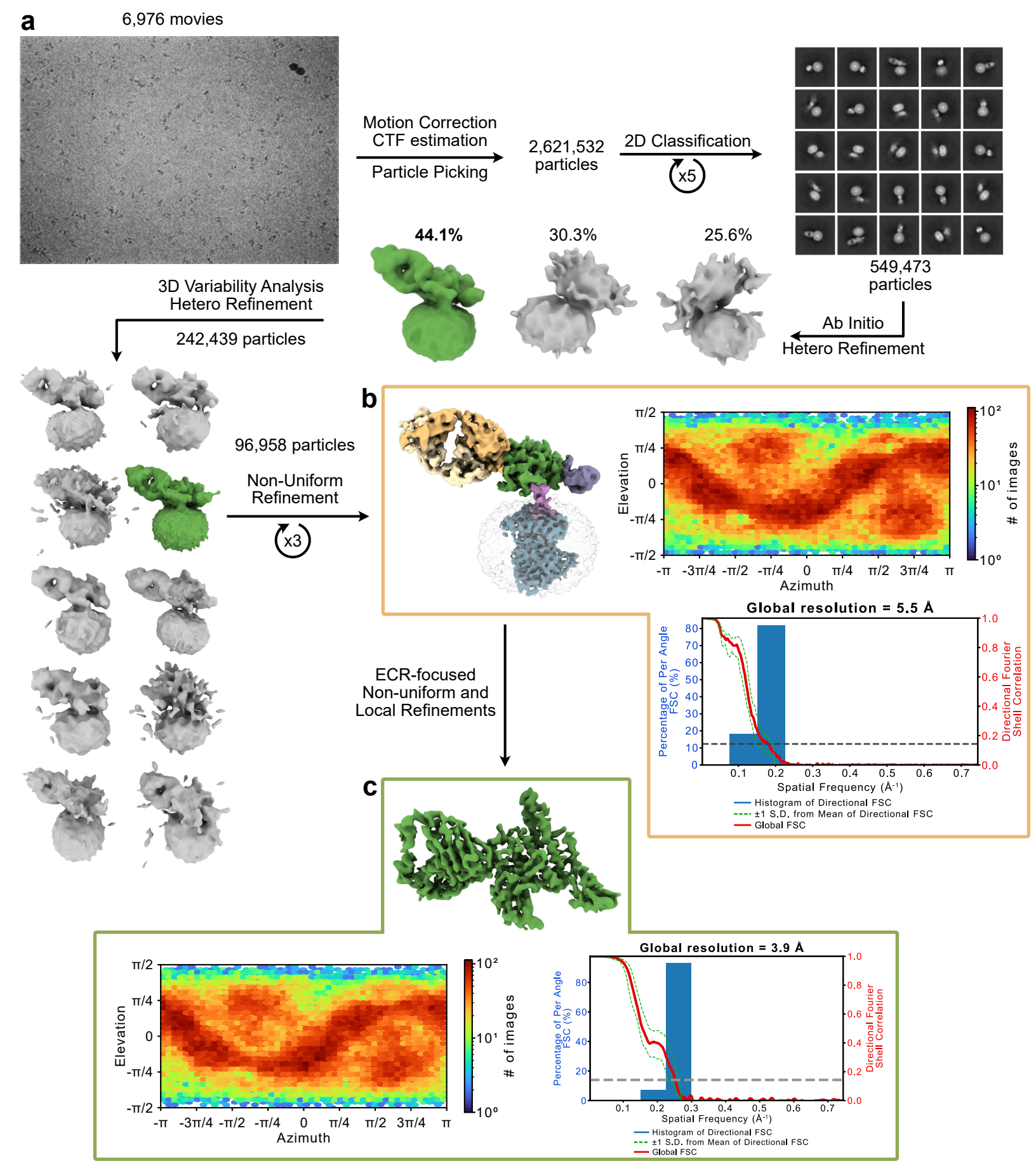

Supplementary Fig. 3: Cryo-EM data processing of HormR+GAIN/7TM ADGRL3.

a Flow chart of cryo-EM data processing and cryo-EM maps of ADGRL3 holoreceptor. **b** 5.5 Å map of ADGRL3 holoreceptor with a graph presenting angular distribution of particles used in the final 3D reconstruction and gold-standard Fourier shell correlation curves of the refinement. **c** Final 3.9 Å map of ADGRL3 HormR/GAIN domains in complex with sAB LK3. Below, a graph presenting angular distribution of particles used in the final 3D reconstruction and gold-standard Fourier shell correlation curves of the refinement.

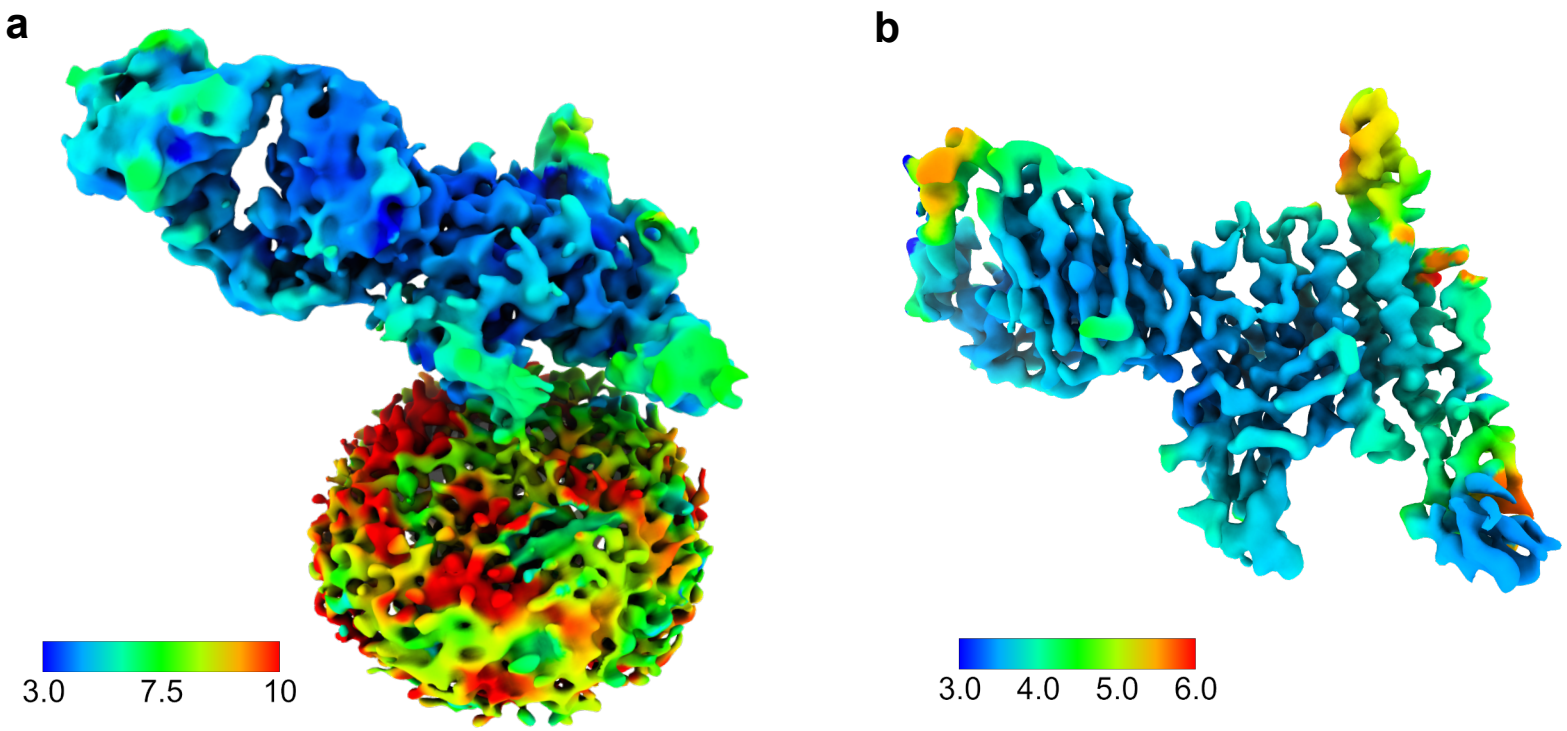

Supplementary Fig. 4: 3D Cryo-EM maps of ADGRL3 colored by local resolution.
A local resolution density maps of **a** ADGRL3 holoreceptor in detergent micelle and **b** HormR/GAIN domains in complex with sAB LK3, colored from blue (higher resolution) to red (low resolution).

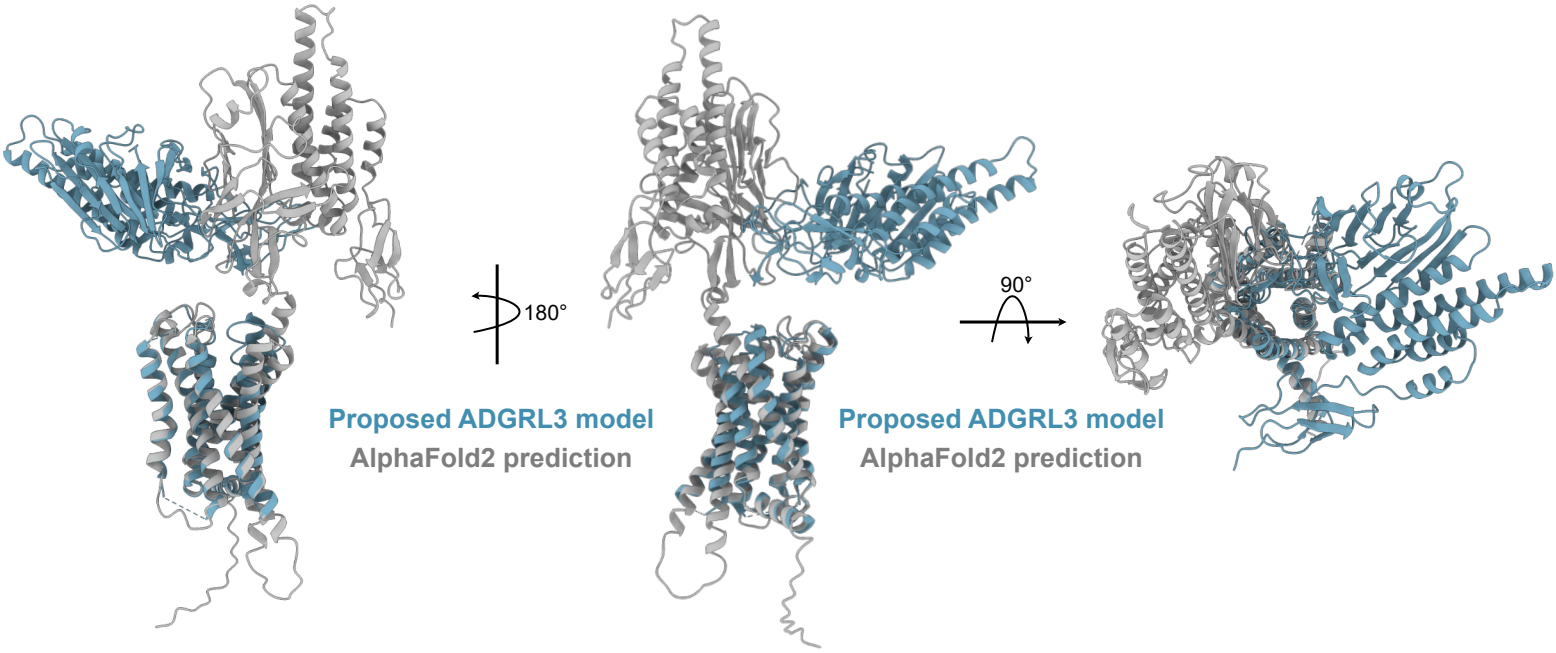

Supplementary Fig 5: Comparison of the hypothetical ADGRL3 HormR+GAIN/7TM model to AlphaFold2 prediction.
Side and top views of proposed ADGRL3 holoreceptor model based on low-resolution cryo-EM map (blue) with the AlphaFold2 prediction of the HormR+GAIN/7TM construct (gray) superimposed over 7TM domain.

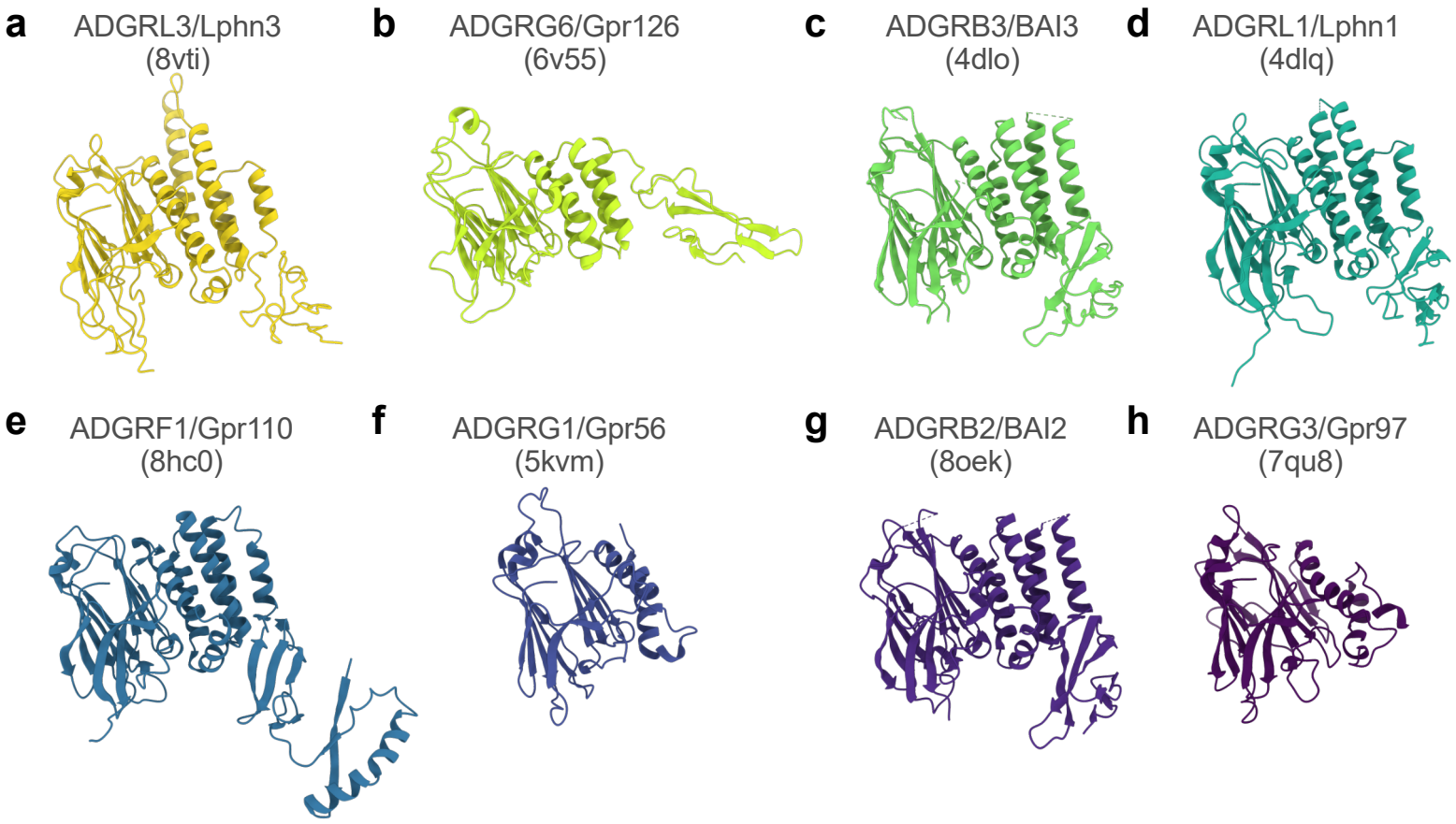

Supplementary Fig 6: Comparison of ADGRL3 HormR+GAIN structure to available structures of GAIN domains of other adhesion GPCRs.

GAIN domain structures of **a** ADGRL3/Lphn3 (PDB: 8vti), **b** ADGRG6/Gpr126 (PDB: 6v55), **c** ADGRB3/BAI3 (PDB: 4dlo), **d** ADGRL1/Lphn1 (PDB: 4dlq), **e** ADGRF1/Gpr110 (PDB: 8hc0), **f** ADGRG1/Gpr56 (PDB: 5kvm) **g** ADGRB2/BAI2 (PDB: 8oek) and **h** ADGRG3/Gpr97 (PDB: 7qu8), presented in the same orientation relative to ADGRL3, show conserved common fold of the domain.

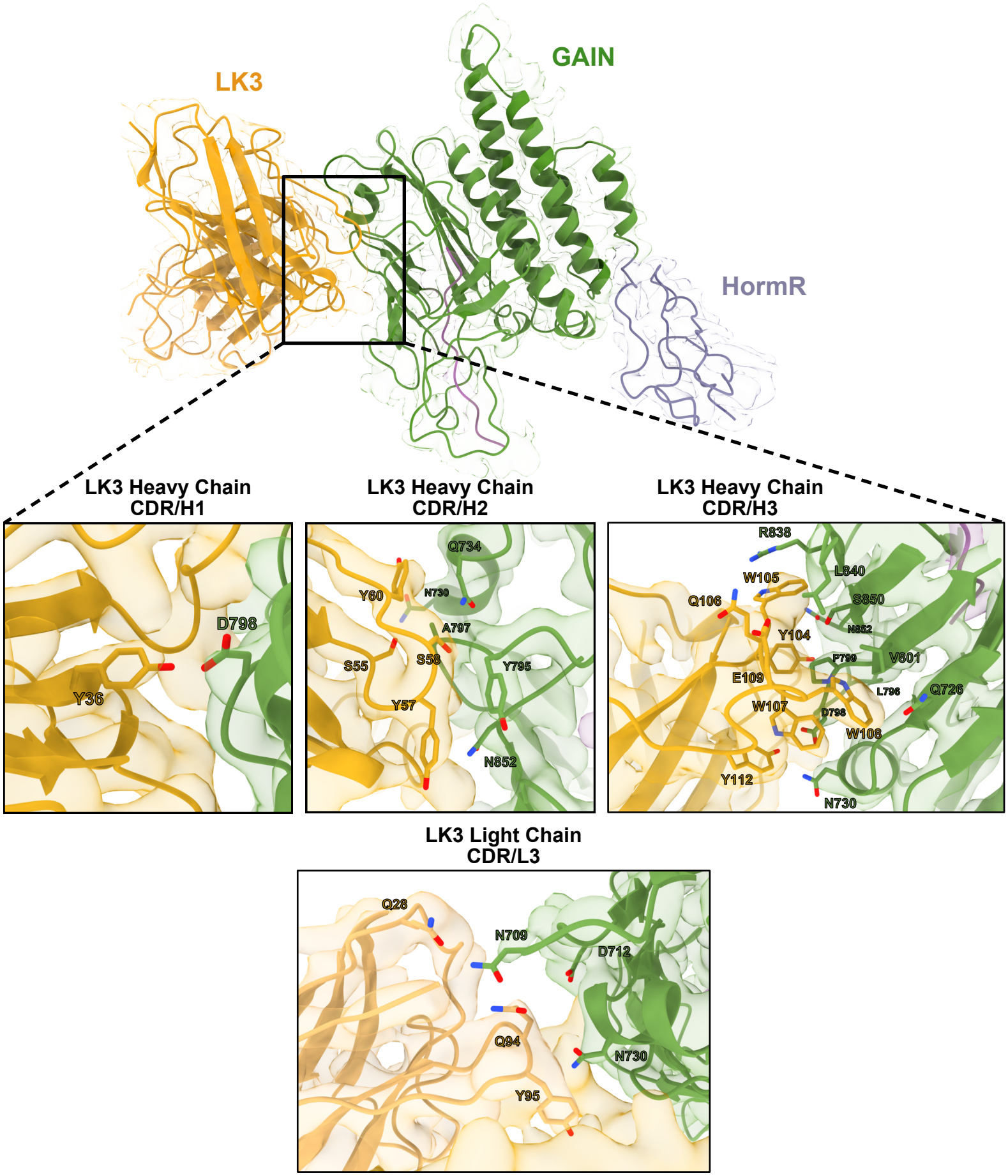

Supplementary Fig. 7: cryo-EM structure of LK3-bound HormR/GAIN domains of ADGRL3.
Model of HormR/GAIN domains of ADGRL3 in complex with sAB LK3 fitted into the cryo-EM map; zoomed-in detailed views of crucial residues from LK3 complementarity-determining regions (CDRs, in yellow) making interactions with residues on GAIN domain of ADGRL3 (green) are shown as sticks.

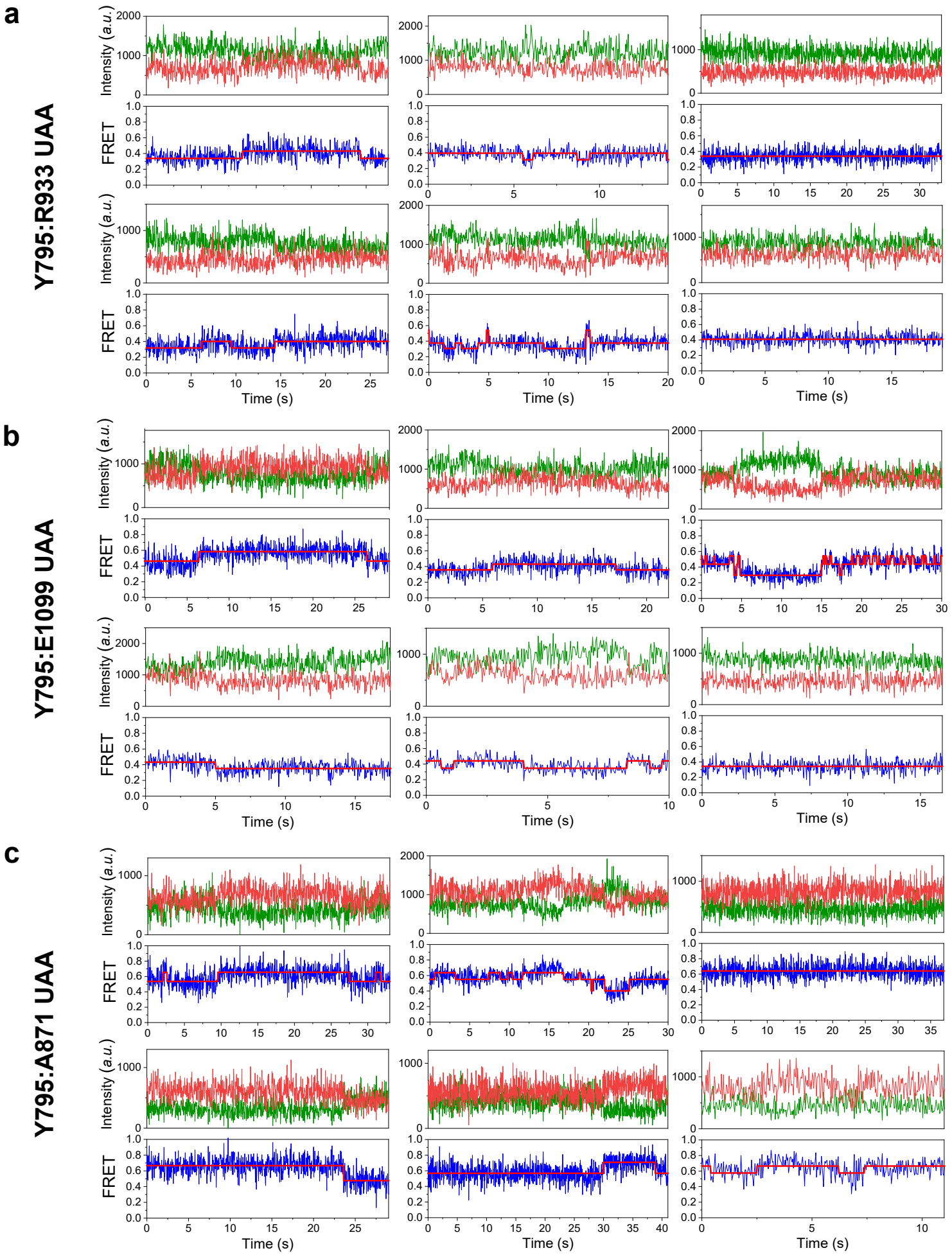

Supplementary Fig. 8: Representative smFRET traces for different sensors.

Representative smFRET traces of **a** Y795:R933 UAA **b** Y795:E1099 UAA **c** Y795:A871 UAA sensors showing traces with a single FRET state, two FRET states, and three FRET states before photobleaching

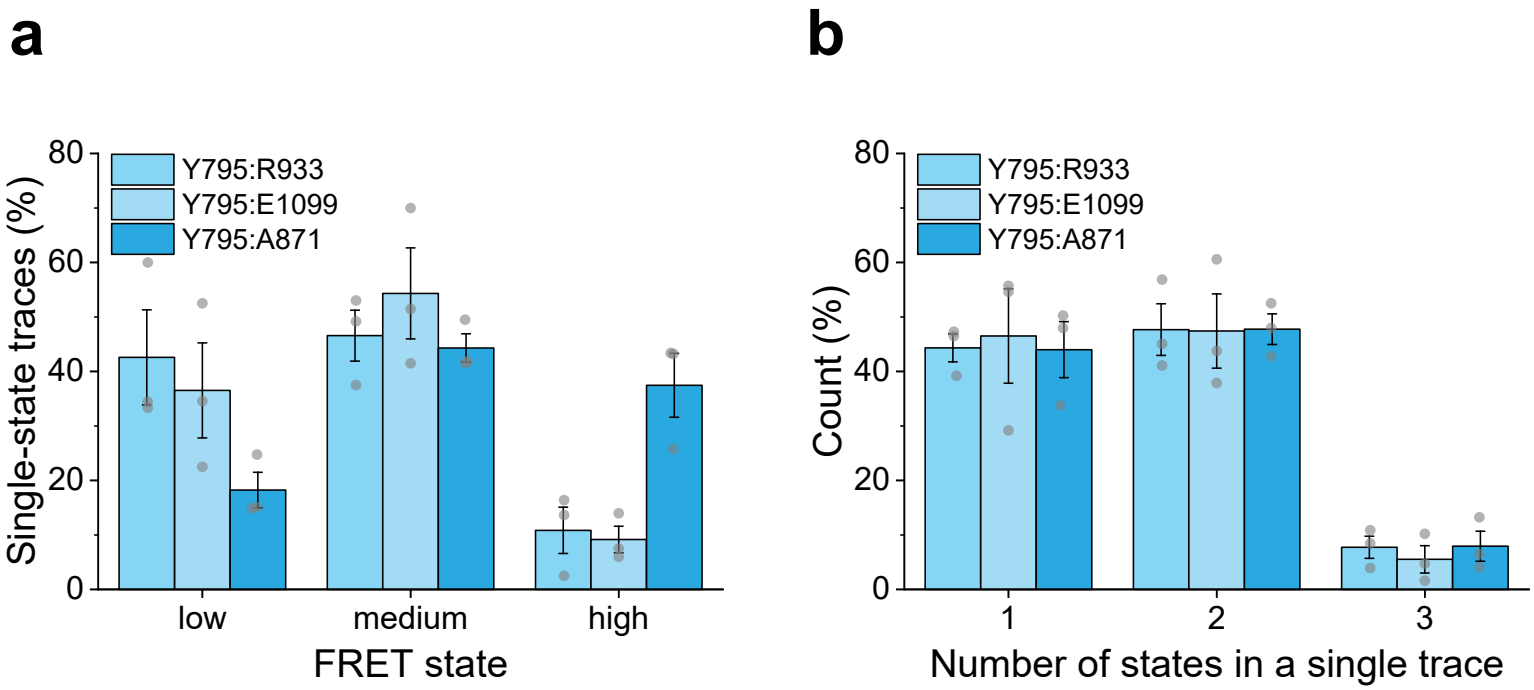

Supplementary Fig. 9: smFRET states and occupancy quantification for sensors.

a Quantification of the occupancy of each FRET state for each of the Y795:R933 UAA, Y795:E1099 UAA, Y795:A871 UAA sensors. **b** Quantification of the number of states in a single trace for each of the Y795:R933 UAA, Y795:E1099 UAA, Y795:A871 UAA sensors. **a, b** Data represent mean ± s.e.m. (*n* = *3*), of three independent biological replicates.

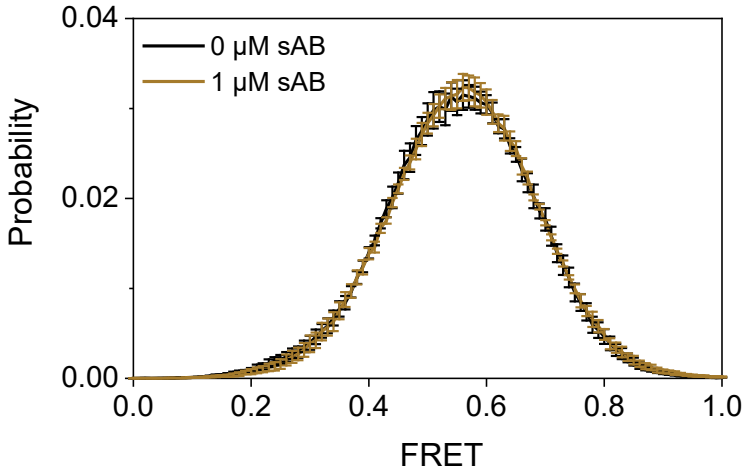

Supplementary Fig. 10: smFRET population histogram in the absence and presence of 1 μM of non-specific synthetic antibody fragment.

Control experiment with 1 μM of non-binding sAB showing no change in the smFRET histogram. Data represent mean ± s.e.m. (*n* = *2*), of two independent biological replicates.

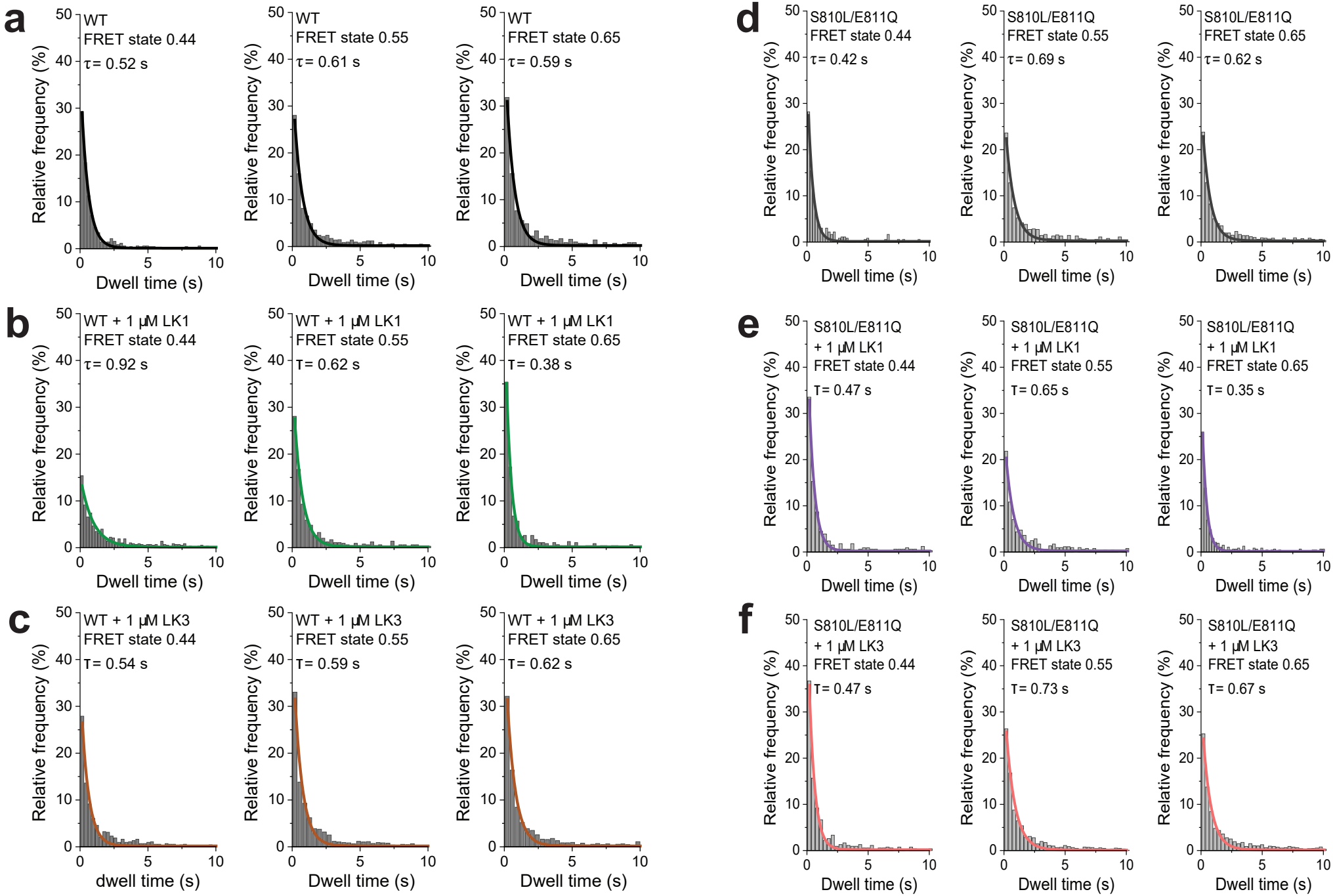

Supplementary Fig. 11: Dwell time analysis for the ADGRL3 WT and S810L/E811Q cancer mutant.

Dwell times of FRET states 0.44, 0.55 and 0.65 (Y795:A871 UAA sensor) for: **a, b, c** WT receptor - (**a)** control conditions, (**b)** addition of 1 μM LK1, (**c)** addition of 1 μM LK3; and **d, e, f** S810L/E811Q cancer mutant - (**d)** control conditions, (**e)** addition of 1 μM LK1, (**f)** addition of 1 μM LK3. Single exponential decay function was fitted to the data to calculate the average dwell time for each condition. Dwell times of fitted states represent the mean of at least two independent biological experiments.

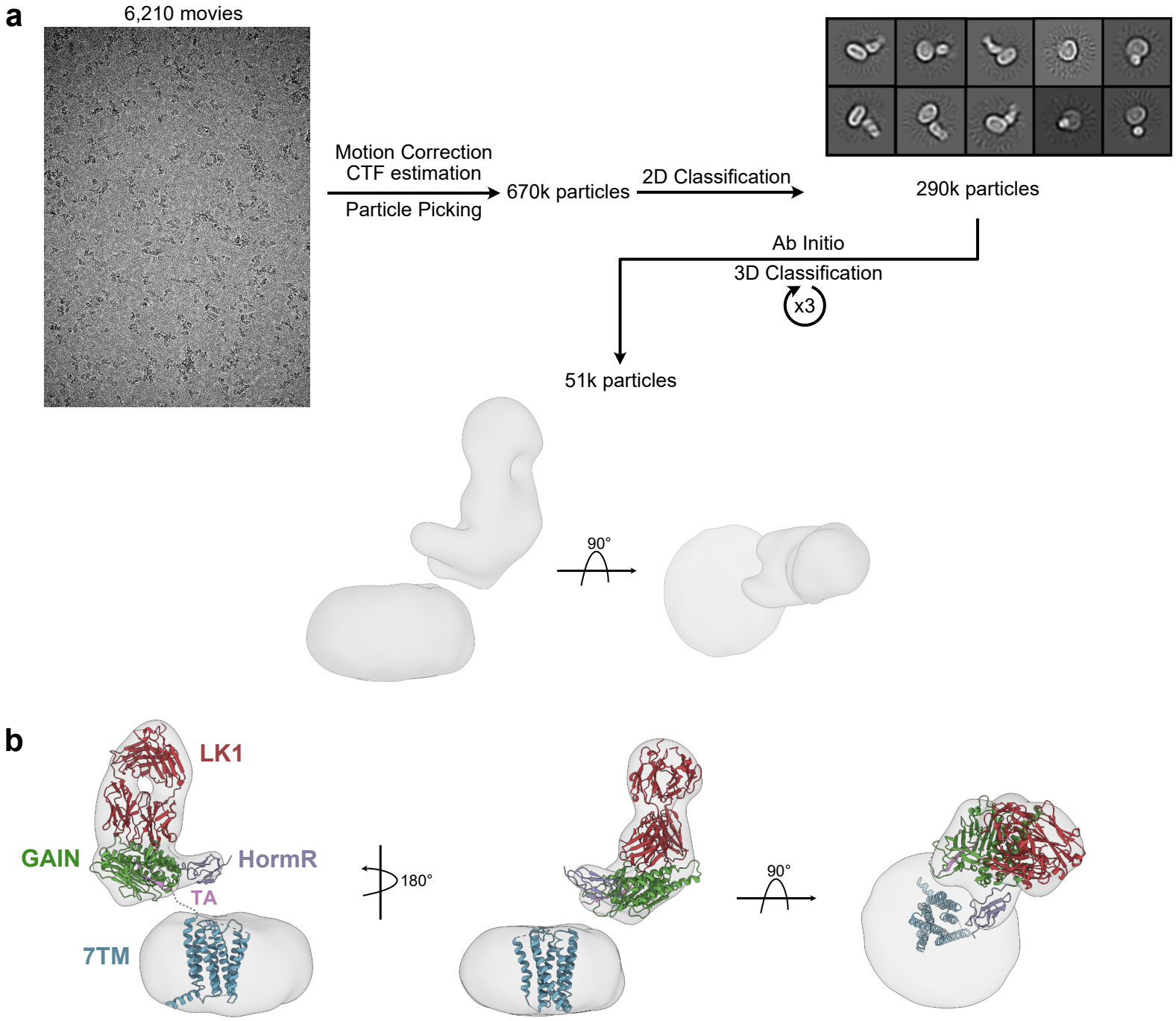

Supplementary Fig. 12: Cryo-EM data processing of ADGRL3/LK1 complex.

a Flow chart of cryo-EM data processing of ADGRL3/LK1 complex. **b** Low resolution 3D map of ADGRL3 receptor in complex with sAB LK1 with docked available structures of the ADGRL3 HormR/GAIN domains, 7TM region (PDB: 8jmt), and sAB (PDB: 8djg).

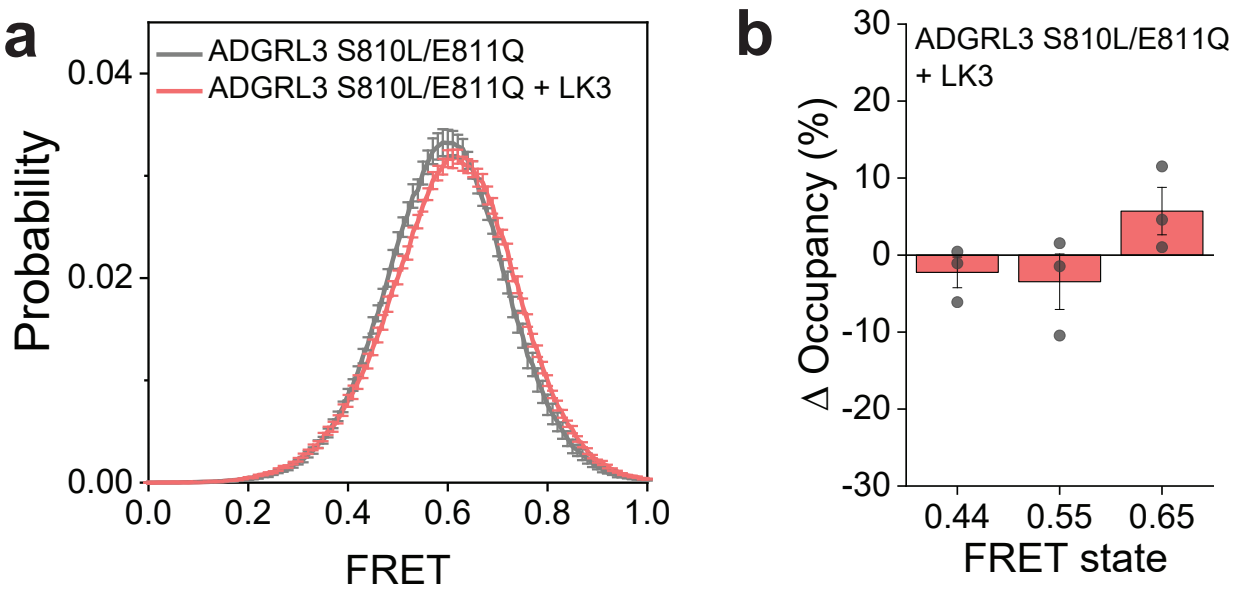

Supplementary Fig. 13: smFRET population histogram in the absence and presence of 1 µM of neutral binder LK3.

a smFRET population histogram for ADGRL3 mutant S810L/E811Q with or without 1 µM LK3. **b** Change in the occupancy of the three FRET states after addition of 1 µM LK3 to ADGRL3 mutant S810L/E811Q. **a, b** Data represent mean ± s.e.m. (*n* = *3*), of three independent biological replicates.

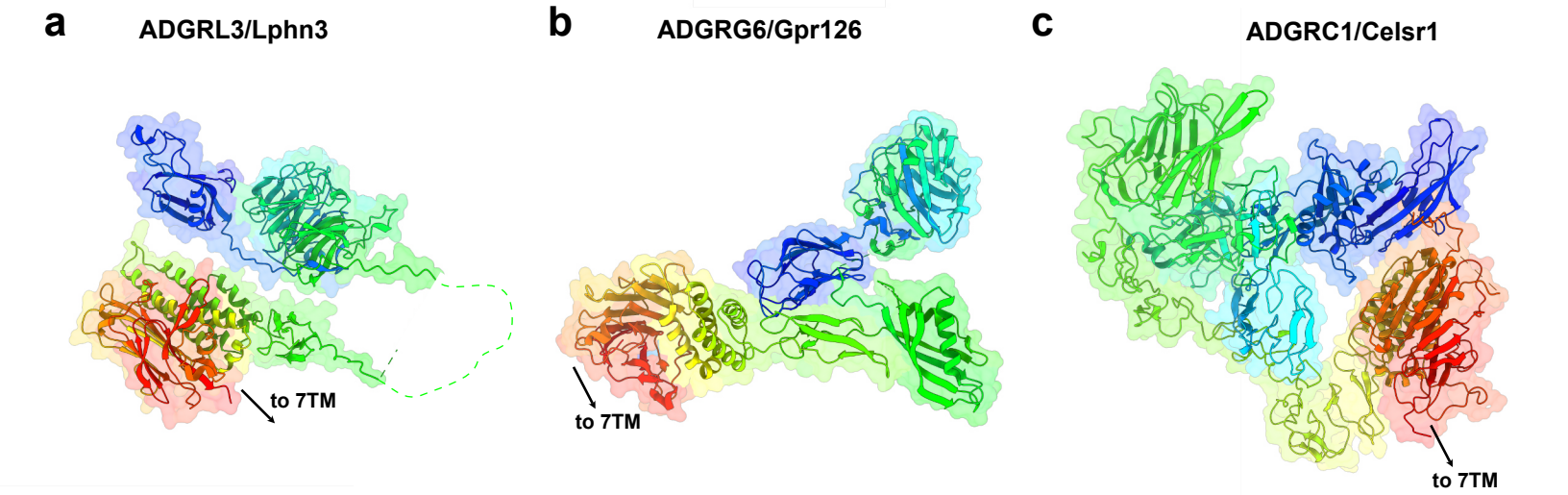

Supplementary Fig. 14: aGPCRs adopt compact conformations of their extracellular regions.
a AlphaFold prediction of ADGRL3 full-length ECR conformation. **b** X-ray crystallography structure of FL ECR of ADGRG6/Gpr126 (PDB: 6v55). **c** cryo-EM structure of C-terminal fragment of ECR of ADGRC1/CELSR1. Presented models, colored from blue (N-terminus) to red (C-terminus), show that ECRs of aGPCRs can form a compact multidomain modules.

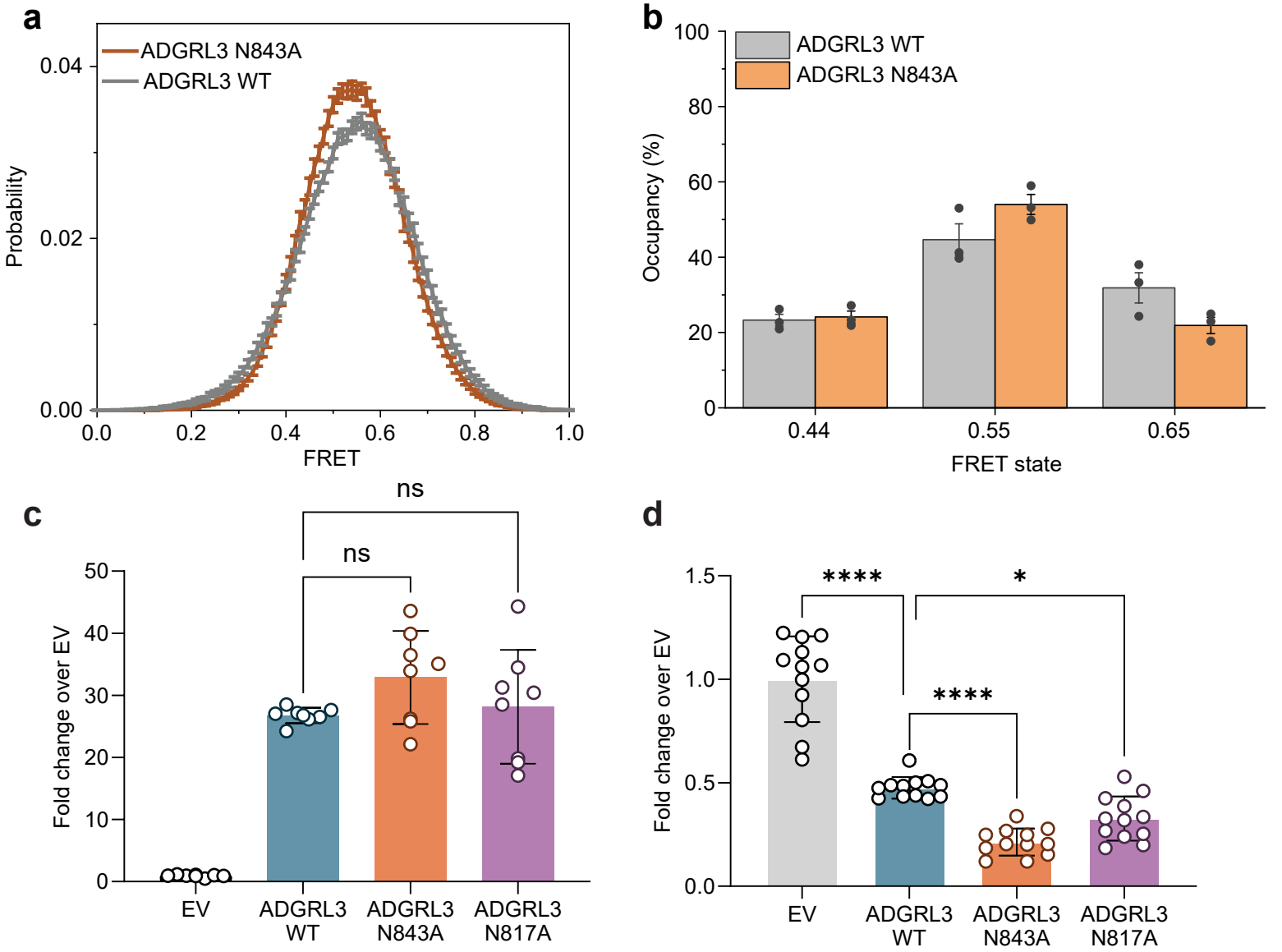

Supplementary Fig. 15: Analysis of ADGRL3 glycosylation mutants by smFRET and signaling assays.
a smFRET population histogram for ADGRL3 mutant N843A and WT receptor. **b** State occupancy (%) of the three FRET states of N843A mutant and WT ADGRL3. **a, b** Data represent mean ± s.e.m. (*n* = *3*), of three independent biological replicates. **c** $ADGRL3_{WT}$ and ADGRL3 glycosylation mutants signaling measured by the SRE-luciferase assay. Data are shown as a fold change over EV. Data are presented as mean ± SD of three independent experiments (n = 8); one-way ANOVA. **d** $ADGRL3_{WT}$ and ADGRL3 glycosylation mutants signaling measured by the cAMP assay. Data are shown as a fold change over EV in the ADRB2 background. Data are presented as mean ± SD of three independent experiments (n = 12); one-way ANOVA.

Supplementary Table 1. Cryo-EM data collection and refinement statistics.

	ADGRL3 HormR/GAIN + LK3 complex	ADGRL3 HormR/GAIN/7TM + LK3 complex	ADGRL3 HormR/GAIN/7TM + LK1 complex
Data Collection and Processing			
Magnification (×)	64,000	64,000	81,000
Voltage (kV)	300	300	300
Electron Exposure ($e^-/Å^2$)	65	65	50.7
Exposures	6976	6976	6210
Defocus range (μm)	-1.0 to -2.0	-1.0 to -2.0	-1.4 to -2.4
Pixel Size (Å)	0.67	0.67	0.561
Symmetry Imposed	C1	C1	C1
Reconstruction			
Initial Particle images	2,621,532	2,621,532	670,000
Final Particle images	96,958	96,958	51,286
Global Resolution (Å)	3.9	5.5	-
Resolution Range (Å)	3.0-7.0	3.0-15.0	-
Map Sharpening B factor ($Å^2$)	-157.7	-80.7	-
Model Composition			
Non-hydrogen atoms	4667	-	-
Protein Residues	596	-	-
Ligands	4	-	-
B Factors			
Protein ($Å^2$)	112.46/208.29/162.40	-	-
Ligand ($Å^2$)	142.68/233.99/190.58	-	-
R.M.S. deviations			
Bond lengths (Å)	0.012 (0)	-	-
Bond Angles (º)	1.472 (11)	-	-
Validation			
MolProbity Score	2.29	-	-
Clashscore	6.19	-	-
Rotamer outliers (%)	3.54	-	-
Ramachandran Plot			
Favored (%)	91	-	-
Allowed (%)	9	-	-
Disallowed (%)	0	-	-

.